Rapid change in plankton community structure during spring along the eastern Beagle Channel

Andreana Cadaillon, Clara M. Iachetti, Ricardo Giesecke, Valeska Vásquez Lepio, Andrea Malits, Irene R. Schloss

PII: S0924-7963(23)00050-7

DOI: https://doi.org/10.1016/j.jmarsys.2023.103906

Reference: MARSYS 103906

To appear in: *Journal of Marine Systems*

Received date: 8 August 2022

Revised date: 21 April 2023

Accepted date: 4 May 2023

Please cite this article as: A. Cadaillon, C.M. Iachetti, R. Giesecke, et al., Rapid change in plankton community structure during spring along the eastern Beagle Channel, *Journal of Marine Systems* (2023), https://doi.org/10.1016/j.jmarsys.2023.103906

Rapid change in plankton community structure during spring along the eastern Beagle Channel

Andreana Cadaillon[*,1], Clara M. Iachetti[*,1], Ricardo Giesecke[2,3], Valeska Vásquez Lepio[2,3], Andrea Malits[1,4], Irene R. Schloss[1,5,6]

[1] Laboratorio de Oceanografía Biológica, Centro Austral de Investigaciones Científicas (CADIC-CONICET), Ushuaia, Argentina.

[2] Instituto de Ciencias Marinas y Limnológicas, Universidad Austral de Chile. Independencia 631, Valdivia, Chile.

[3] Centro de Investigación en Ecosistemas Marinos de Altas Latitudes (IDEAL), Valdivia, Chile.

[4] Department of Functional and Evolutionary Biology, University of Vienna, Austria

[5] Instituto Antártico Argentino, Buenos Aires, Argentina

[6] Instituto de Ciencias Polares y Ambiente, Universidad Nacional de Tierra del Fuego Ushuaia, Argentina.

*Joint first authors

Corresponding author: claraiachetti@gmail.com

ABSTRACT

In November 2019, a first joint Chilean–Argentinian research cruise was conducted along the eastern section of the Beagle Channel (BC). Here we present the results of the microbial plankton (2–200 µm cell size) abundance and composition analyses in relation to water masses and environmental variables, along a longitudinal transect characterized by contrasting hydrology. Plankton samples were analyzed within the photic zone along the channel and at two fixed stations during two short time series (a first one of 30 and a second one of 42 h). Results revealed a spatial zonation in the composition and structure of the plankton assemblages, related to bathymetry, water temperature and nutrient availability but also, a small-scale temporal variability due mainly to a rise in air and water temperature. The inner (westernmost) and outer sectors of the sampled area, west and east of Mackinlay Strait, respectively, were characterized by low plankton abundances, mostly dominated by nanoflagellates and some large diatoms. In contrast, the easternmost sector of BC, showed the highest total cell abundances, displaying a high diversity of small and large diatoms. Notably, in the inner BC (fixed station F1), chl-*a* concentrations almost doubled in 24 hours, along with an increase in total plankton abundance and the dominance of small diatoms and

nanoflagellates. Rapid changes in plankton relative abundance were also observed east to Mackinlay Strait. This highlights the large spatial (km) and temporal (hours to days) plankton heterogeneity along the eastern section of the BC, scales which should be considered for further sampling strategies.

1.INTRODUCTION

It is well established that phytoplankton dynamics are shaped by fluctuations at different temporal scales (Harris 1980; Reynolds, 1990): from semidiurnal tidal cycles, diurnal cycles in light (Cloern, 1991; Lucas and Cloern, 2002; Wetz et al., 2006, Leles et al., 2014), seasonal changes in light, temperature, stratification, and nutrients (Almandoz et al., 2011; Iriarte et al., 2018), to interannual, long-term climate variability (Alvarez-Cobelas et al., 2019, Harris et al., 2014). In subantarctic environments, the physical and chemical environment may vary rapidly in temporal but also small-scale spatial variation (Swart et al., 2015; Thomalla et al., 2011). Wind storms (Iriarte et al., 2001; Carranza and Gille 2014) and heavy precipitation (Käse and Geyer, 2018) as well as calm weather accompanied by high radiation (Boyd, 2002; Arrigo et al., 2008) could therefore alter the typical phytoplankton succession pattern modulating phytoplankton communities, especially during the spring-summer season. The subantarctic BC is a semi-estuarine system connecting the Pacific and Atlantic Oceans. The BC shows marked hydro-meteorological seasonal cycles, with air temperatures between 5 and 14 ºC during austral summer, when the prevailing Southwest winds are intensified (Garreaud et al., 2009), and temperatures between -1 and 5 ºC during winter (Iturraspe et al., 1989). The main hydrographic features include a dominant west to east circulation influenced by Subantarctic Waters (SAAW), the Cape Horn Current, and a strong spatial gradient in freshwater discharge (Giesecke et al., 2021). An intricate bottom bathymetry, with depths varying from 644 m depth on the western Pacific side (Balestrini et al., 1998) to ~40 m depth on the eastern, Atlantic side (Valdenegro and Silva, 2003), separates the channel into several microbasins. Surface salinities increase in winter and decrease in spring-summer due to freshwater input, driving water column stratification and the formation of a seasonal pycnocline at around 60 m (Giesecke et al., 2021). The tidal regime is mixed semidiurnal with average tidal amplitudes of 1.2 m, ranging from 0.67 to 2.18 m (Balestrini et al., 1998).

In November 2019, a joint Chilean-Argentinian cruise along the eastern section of the BC addressed the question of how meteorological, physical and chemical variables influence the distribution of plankton community' structure, size-fractions, composition and abundance along the BC during austral spring on both the spatial and short-term

(from hours to days) temporal scale. We hypothesize that rapid variations in environmental conditions could lead to an identifiable short term-response in plankton composition, related to the combination of changing meteorological and hydrographical conditions. To test this, here we assess the microbial plankton structure (2–200 µm cell size organisms) in terms of species composition, size-fraction groups, and abundance both across a longitudinal transect and at two fixed stations (in the inner and outer BC, according to Iachetti et al., 2021). This allows us to analyze the temporal and spatial scales of plankton variability along the eastern section of the BC (east of 68.6º W). This study further provides contextual information about plankton abundance and composition to other works in the Special Issue on the Binational Cruise in the BC.

2. MATERIALS AND METHODS

2.1. Field work and sample processing

From November 9 to 15, 2019, the first binational Chilean-Argentinian expedition along the BC was conducted onboard the R/V *Victor Angelescu.* Eight discrete stations were sampled along a longitudinal W-E transect (Fig. 1). Two additional fixed stations were sampled every 6 hours for 42 h at F1 (54°53.32'S, 67°46.92'W) and 30 h at F2 (54°54.03'S, 67°16.31'W), west and east of Mackinlay Strait, respectively. Fixed stations were performed following the semidiurnal tidal cycle.

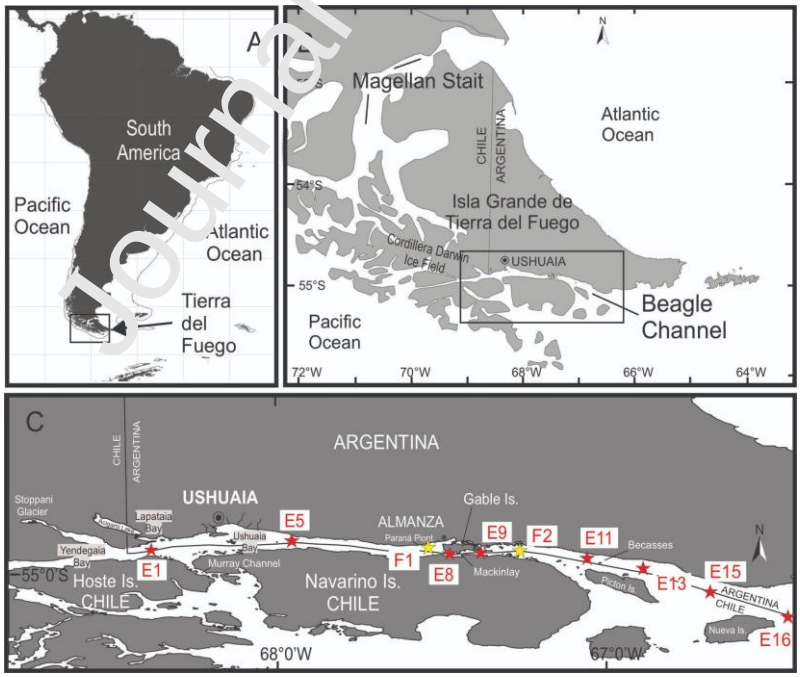

Figure 1. Location of the study area in the southern tip of South America (A), Tierra del Fuego (B) and study area with the sampled stations (C) along the W to E transect (red stars) and fixed stations, sampled on the way back (yellow stars). The solid black line indicates the Argentine-Chilean border. 1/3 PAGE

2.2. Physical and chemical variables

At each station and during each of the sampling events at the fixed stations F1 and F2, a SeaBird SBE-9 CTD was deployed for vertical profiling and discrete water sampling. The CTD was additionally fitted with auxiliary sensors of oxygen, PAR, and fluorometry, and was attached to twelve 8 L Niskin bottles (SBE-32 rosette) for water sampling. In addition, underway surface (4 m) seawater temperature data were continuously measured by means of a Seabird SBE 38 CTD. Water samples were collected at surface (5 m, 22 samples), chlorophyll-*a* (chl-*a*) maximum (10 to 32 m) and at ~10 meters from the bottom, for later analysis of dissolved inorganic nutrients (nitrate+nitrite, phosphate and silicic acid) at IFOP's Center for Harmful Algae Studies (CREAN), using Seal Analytical AQ-400 autoanalyzer (Mequon, WI, USA) according to international standard techniques (EPA, 2000; APHA / AWWA / WEF, 1999, 2000; USEPA, 1983, 1993; for more details see Schloss et al., 2023). Data between the surface and the maximum of chl-*a* will be used in the present study.

2.3. Biological parameters

2.3.1. Total and size-fractionated chlorophyll-*a*

For total chl-*a* (chl-a_{TOT}) determination, 200 mL seawater subsamples from each depth were filtered onto GF/F filters (0.7 µm nominal pore size) in triplicate and kept frozen at -80°C until analysis. Size-fractionated chl-*a* subsamples were obtained by three sequential steps; 500 mL of seawater were prefiltered through a 20 µm nitex mesh and the eluted water was sequentially filtered through 2 µm nucleopore (chl-*a* 2-20 µm, nanoplankton fraction) and 0.7 µm GF/F filters (chl-*a* 0.7-2 µm, picoplankton fraction). Chl-*a* >20 µm (microplankton fraction) was determined as the difference between chl-a_{TOT} and the other size-fractions (Iriarte et al., 2000; Gonález et al., 2010, 2016; Jacob et al., 2014). Chl-a_{TOT} and size-fraction chlorophyll were extracted during 24 h in cold and dark conditions with 90 % acetone and determined with fluorometry (Trilogy, Turner Design), according to standard procedures (Parsons et al., 1984).

2.3.2. Diversity of the eukaryotic unicellular nano- and microplankton

At all stations Seawater samples (100 mL) for nano- and microplankton qualitative analyses were collected on vertical net tows (20 m to surface) using a 25 µm mesh net. Samples were fixed with formaldehyde neutralized with Borax (4 % final concentration) and examined using a Leica DM2500 optical microscope equipped with phase contrast.

For nano- and microplankton quantitative analysis, seawater subsamples (250 mL) from depths mentioned above (see 2.2) were fixed with acidic Lugol's solution at 2 %

final concentration (Alder and Morales, 2009) and stored in the dark at 4 °C until analysis. Eukaryotic cells >2 µm were identified to the lowest possible taxonomic level according to Tomas (1997) and regional references (Almandoz et al., 2011; Iachetti, 2018; Guinder et al., 2020). At least 300 cells were counted with an IROSCOPE inverted microscope SI_PH922394 according to Utermhöl (1958). For colonial individuals, the number of cells in a colony were counted. Plankton abundance was then expressed in cell L^{-1}. In the present study, the term plankton refers to the size range >2 µm, that could be identified using optical microscopes.

2.4. Data analysis

For data analysis, stations were grouped according to Iachetti et al. (2021), who established two well defined hydrological sectors according to their bathymetry and environmental conditions, separated by the Mackinlay Strait; the inner BC (E1, E5, E8, F1) and the outer BC (E9, E11, E13, F2). The easternmost stations (E15, E16), beyond Picton Island, were not considered by Iachetti et al. (2021), thus hereafter referred to as "mouth" of BC (see description in results).

Hourly data of meteorological variables, i.e. air temperature (T_{AIR}), wind speed and direction were provided by the Global Atmospheric Watch Station (VAG-Ushuaia) located on the Ushuaia Peninsula (54º 50.92′ S, 68º 18.53′ W). For statistical analyses, the average wind-speed and air temperature of the 24 h before the actual sampling times were considered.

The Brunt-Väisälä buoyancy frequency (BV) was calculated at each station; the highest buoyancy frequency value was used as a proxy for the mixed layer depth (MLD; Mann and Lazier, 2013).

CTD fluorometry data were converted into chlorophyll values (CTD-Chlorophyll) by calibration with discrete chlorophyll-*a* concentration values (chl-a_{TOT}) recorded during the cruise. For each station, biological data from only the first two sampling depths (2 to 3 discrete samples were averaged between 5 and 32 m depth) were considered in this publication. For statistical analysis and summary information in Tables 1 and 2, hydrographical variables were processed as follows: for Salinity (S), Seawater Temperature (Tw), Sigma Theta (σ_t) and CTD-chlorophyll, the median was considered, to obtain a robust value with less outlier data influence. For inorganic nutrients, total and discrete size-fractionated chl-*a* and nano- and microplankton abundances, the average value was considered.

Multivariate Principal Component Analysis (PCA) was performed to identify associations between meteorological and hydrographic parameters and spatial ordination patterns among the sampled stations, at a spatial and a temporal scale. Silicic

acid was not included in the analysis as concentrations were below the detection limit (0.64 µmol L^{-1}) in almost all the samples.

Hierarchical Cluster Analysis and a nMDS ordination were performed. Previously, a square root transformation was applied to the biological data to reduce heterogeneity among the different taxa abundance considered, *i.e.*, nano- and micro-sized diatoms, nano and micro-sized dinoflagellates, nano- and micro-sized ciliates, other protists >20 µm (silicoflagellates and euglenophytes) and nanoflagellates (cryptophytes, prasinophytes, prymnesiophytes and unidentified nanoflagellates). An ANOSIM (Clarke and Warwick, 1994) was also carried out to test for statistical grouping between stations. Finally, a symmetrical matrix of all pairwise distances among sampling stations (SIMPER) was calculated with Bray Curtis distance. All statistical analyses were performed using the software PRIMER (Clarke and Gorley, 2006).

3. RESULTS AND DISCUSSION

Results will be presented and discussed considering the spatial variability (8 stations along the W-E transect) and the temporal variability at different scales, from days (*i.e.* comparing sites that were sampled in two different opportunities, during the W-E transect and then again, during the fixed stations) to a few hours (analyzing the fixed stations, sampled every 6 hours for 42 and 36 h).

3.1. Spatial variability

A rise in air temperature (T_{Air}) was observed, varying from 3.25 ºC in the inner BC (stations E1, E5, E8) to 7.63 ºC in the mouth of BC (stations E15 and E16), while at the same time wind speed diminished from 29.92 to 5.16 km h^{-1} on the way East. Accordingly, the highest value of MLD (105 m, Table 1) was observed in the inner BC (particularly in stations E1 and E5), which is also deeper than the rest of the studied region of the channel. The deepening of the MLD could be due to a combination of winds and Venturi effects at Diablo Island (Giesecke et al., 2021), particularly close to the station E1, in which complete homogenization of the water column takes place. This affected biological processes, E5 showing the lowest net community production measured in the transect, as well as the lowest production:respiration rate (Latorre et al., 2023). Wind driven vertical mixing is a very recurrent process, mainly in shallow areas in BC, especially in winter, when water column homogenization can reach the sea bed, even in the deeper microbasins (150 to 200 m, Martin et al., 2016; Flores Melo et al., 2018). In contrast, in the eastern sector of BC, stratification was weak (BV < 18 cycles h^{-1}) and MLD shallow (~7m). Water temperature (T_W) ranged from 6.26 to 6.67 ºC, while

salinity varied from 31.08 to 32.75 (Fig. 2 A-C), the lowest values corresponding to the inner BC for both variables. Water density was determined by salinity (not shown) as previously reported by Martin et al. (2016). No thermal stratification was evident except in E1, where temperature varied from 6.30 ºC in the surface to 5.88 ºC at 80 m, and to 6.65 ºC near the bottom. Salinity stratification was evident in the upper 100 m of the water column, changing from 31.09 to 32.27 in the inner BC (E1) and, in the upper 10 m, changing from ~31.60 (surface) to ~32.22 (near the bottom), in the outer BC (stations E11 and E13, Table 1, Fig. 2 B and C). These features are similar to those previously described for the study area (Flores Melo et al., 2020; Giesecke et al., 2021; Iachetti et al., 2021).

Table 1. Summary of meteorological and hydrological variables during the studied period for eastern Beagle Channel. 24 h-averaged air temperature (T_{AIR}) and wind speed (Wspeed), Median values for water temperature (T_W), salinity (S), density sigma theta (σ_t) and averaged values ± standard deviation for nutrient concentration, for surface to maximum chl-*a* depths (0-32 m) at all sampled stations (longitudinal transect). S.date, sampling date. Bot depth, bottom depth. MLD mix layer depth. MLD: Mixed Layer Depth. nd: Non detectable (<0.64 µmol L^{-1}).

Station	E1	E5	E8	E9	E11	E13	E15	E16
S. date	9-Nov-19	9-Nov-19	9-Nov-19	10-Nov-19	10-Nov-19	10-Nov-19	10-Nov-19	10-Nov-19
Bot. depth (m)	256	155	25	49	110	74	50	28
MLD (m)	105	88	4	8	8	6	9	5
T_{AIR} (ºC)	3.5 ± 1.6	3.2 ± 1.9	4.7 ± 2.1	4.8 ± 1.8	4.7 ± 2.1	5.1 ± 2.7	6.0 ± 3.9	7.6 ± 5.7
W. speed (km h^{-1})	29.9 ± 8.4	25.8 ± 9.8	10.5 ± 10.2	17.2 ± 10.6	7.7 ± 8.3	6.4 ± 6.3	5.2 ± 4.7	5.2 ± 5.1
T_W (ºC)	6.2 ± 0.1	6.3 ± 0.1	6.5 ± 0.0	6.5 ± 0.0	6.5 ± 0.1	6.7 ± 0.1	6.6 ± 0-1	6.5 ± 0.0
S	31.1 ± 0.1	31.2 ± 0.0	31.6 ± 0.0	32.1 ± 0.1	32.1 ± 0.2	32.5 ± 0.1	32.7 ± 0.0	31.1 ± 0.0
σ_t	24.4 ± 0.1	24.5 ± 0.1	24.8 ± 0.0	25.2 ± 0.1	25.2 ± 0.1	25.5 ± 0.1	25.7 ± 0.1	24.4 ± 0.0
PO_4 (µmol L^{-1})	1.4 ± 0.1	1.4 ± 0.4	1.3 ± 0.1	1.1 ± 0.2	1.2 ± 0.2	1.2 ± 0.0	1.3 ± 0.1	1.4 ± 0.0
NO_3+NO_2 (µmol L^{-1})	9.8 ± 0.1	7.3 ± 1.0	6.2 ± 1.5	12.6 ± 7.9	5.6 ± 0.6	8.4 ± 0.2	10.8 ± 0.9	7.4 ± 0.6
N:P	7.3 ± 0.7	5.4 ± 2.1	4.7 ± 1.2	10.8 ± 1.2	4.7 ± 0.3	6.9 ± 0.2	8.4 ± 1.0	5.3 ± 0.5
SiO_4 (µmol L^{-1})	nd	nd	5.46	nd	nd	nd	nd	nd

Nitrate+nitrite (NO_3 + NO_2) and phosphate (PO_4) concentrations (Table 1) averaged 8.53 ± 2.4 and 1.28 ± 0-.11 µM, respectively, with an average N:P ratio of 6.69 ± 2.11. Although no W-E gradient was observed, phosphate concentration showed higher values on the western sector of the transect (Table 1). Concentration values registered on this study are within ranges previously described for the BC at this time of the year

(Giesecke et al., 2021; Iachetti et al., 2021 and references therein). Silicic acid concentrations, as observed in previous studies (Iachetti et al., 2021), were low (<5.46 µM) or even under detection limit (as in 87 % of the analyzed samples) above the chl-*a* maximum depth and all along the transect (Table 1). In the Inner BC (E1 and E5), Silicic acid was only detectable in near bottom samples (at 263 and 146 m, respectively; not included in this study). This would lead to the hypothesis that if intense winds mixed the water column to those depths, silicates could reach surface waters. This was the case in Station E8 in Mackinlay Strait, the only station in which silicic acid concentration (5.5 µmol L^{-1}) above the chl-*a* maximum depth was above the detection limit (0.64 µmol L^{-1}). Relatively high wind speeds were registered during that day and sampling time (around 20 km h^{-1}, Table 1), and given the shallow bottom depth at E8 (25 m, Table 1), the measurable silicic acid concentration was probably related to dissolved nutrients resuspension, as observed in different regions during short wind events (Thyseen et al., 2008, Yeager et al., 2005).

The low nutrient concentrations were most probably responsible for the generally low chlorophyll-*a* concentrations measured (see below), which were *ca*. 6 times lower than previously reported for the region (Iachetti et al., 2021 and references therein) for the same spring months.

Maximum CTD chlorophyll-*a* concentration distribution was generally found between 10-20 m depth (Fig. 2 D).

The spatial variability along the transect was also reflected in the multivariate analysis (PCA, Fig. 3) in which the two first components accounted for 79.9 % of total variability. The eastern BC stations, characterized mainly by higher salinity (stations E11, E13 (as in Giesecke et al., 2021; Iachetti et al., 2021) and stations E15, E16 in the "mouth" of BC) were grouped together but separated from the rest, which presented intermediate conditions and mostly corresponded to the MacKinley Strait (E8 and E9) or the inner channel (E1 and E5). Higher salinity and chl-a_{TOT} values (see below) in this area are likely related to the intrusion of oceanic waters from the Cape Horn Current, reaching the easternmost section of the BC through and around Nueva and Lennox Islands (Acha et al., 2004; Cardona Garzón et al., 2016).

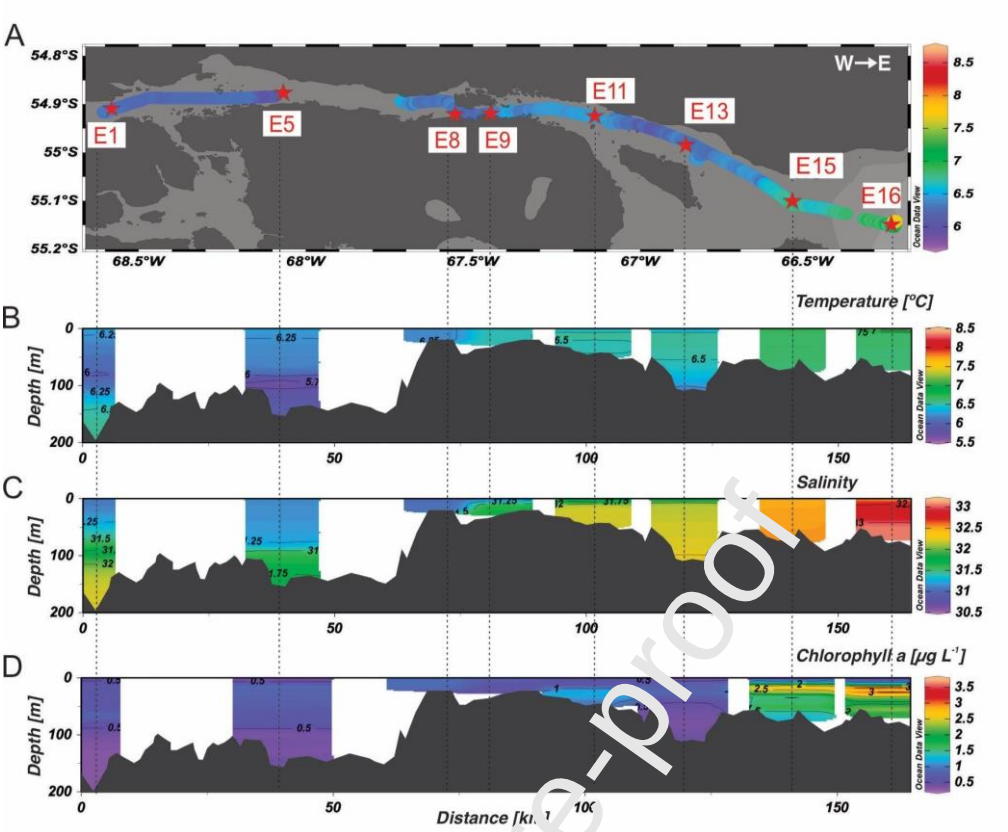

Figure 2. Continuous underway surface water temperature (A) and profiles for (B) water temperature (ºC), (C) salinity and (D) CTD-chlorophyll-*a* (µg L^{-1}), based on calibrated fluorescence data, for all the sampled stations along the W to E transect. 1/3 PAGE

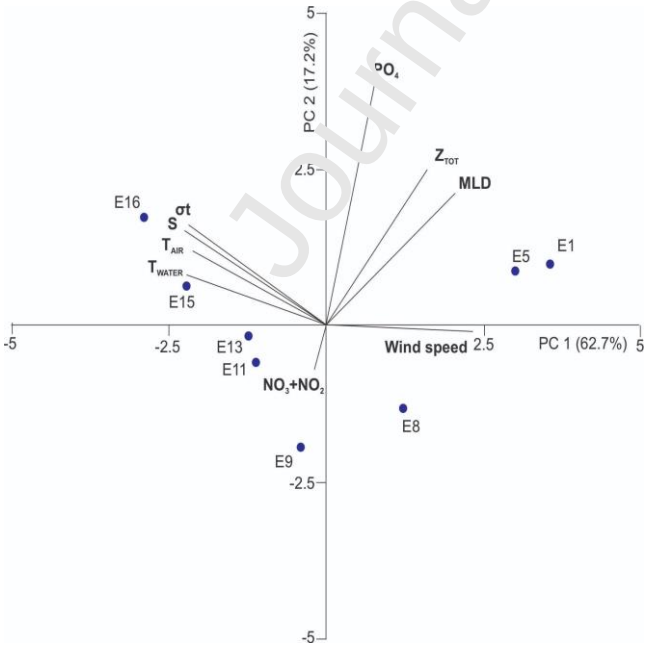

Figure 3. Principal Component Analysis (PCA) scatter plot based on medians and averages of physical and chemical (surface to maximum-Chl-*a* depth) and

meteorological variables for all stations. S: salinity, T_{AIR}: air temperature, T_{WATER}: water temperature, Z_{TOT}: Bottom depth, σ_t: density. MLD: Mixed Layer Depth. COLUMN

Discrete chl-a_{TOT} concentrations from surface to maximum Chl-a depth were generally low along the studied area (< 1.2 µg L^{-1}), with the highest values in the easternmost stations E15 and E16 (2.73 and 2.56 µgchl-*a* L^{-1}, respectively, Fig. 4 A), decreasing with depth. Chl-a_{TOT} was mainly represented by microphytoplankton (chl-$a_{>20µm}$, 50-75 %) in most of the stations, followed by the nanophytoplankton (chl-$a_{2\text{-}20µm}$, 15-30 %) and picophytoplankton (chl-$a_{0.7\text{-}2µm}$, 10-20 %) fractions, except for E1 where pico- and nanophytoplankton were the most important size fractions (40 % and 37 %, respectively), with a low contribution of microphytoplankton (23 %) (Fig. 4A). Microphytoplankton was mainly represented by diatoms, a common feature in the spring summer blooms in both northern subpolar environments (Savidge et al., 1995; Uitz et al., 2009; Irion et al., 2021; Mojica et al., 2015; Ward et al., 2016) and subantarctic areas (Iriarte et al., 2001; Cuevas et al., 2019; Almandoz et al., 2011; Guinder et al., 2020). Total plankton cell abundance >2 µm ranged between $5.8x10^5$ to $2.8\ x10^6$ cell L^{-1}, following a spatial pattern similar to that of Chl-a_{TOT}, reaching the highest values at the mouth of BC.

Along all the sampled stations, from the analyzed planktonic groups, nanoplankton was the dominant size fraction in terms of cell counts being *ca.* 18 times more abundant than microplankton (Fig. 4 B and C). Regarding nanoplankton, cryptophytes, prasinophytes and prymnesiophytes were the less abundant groups and, therefore, were grouped together with the unidentified nanoflagellates as a single group: “Nanoflagellates”.

In the inner BC, stations E1 and E5 nanoflagellates accounted for more than 78 % and diatoms for less than 20 % of total nanoplankton. Dinoflagellates and ciliates < 20 µm accounted for less than 5 % of total nanoplankton abundance (Fig. 4 B). In the Mackinlay Strait (E8 and E9), plankton analysis at E9 was similar to E1 and E5, but E8 showed the highest nanoplankton abundance, presenting similar proportions of diatoms and nanoflagellates (48.5 and 49.4 %, respectively). Mackinlay Stait stations showed intermediate (transitional) environmental conditions between inner and outer BC, and therefore, community composition and abundance seem to be transitional as well. However, for the microbial community, these transitional stations clustered together with those of the east of Mackinlay Strait (as in Malits et al., 2023). For the inner BC and Mackinlay Strait, microplankton (Fig. 4 C) was mainly represented by diatoms (55-97 %). Diatoms were followed in abundance by dinoflagellates (5-30 %), silicoflagellates and

euglenophytes were the less important groups in terms of their contribution to total plankton abundance and were grouped as “Other Protists >20 µm” (Fig. 4 C).

Despite of being a systems with severe silicic acid limitations with ~11 to 19 times less SiOH for, optimal diatom development (N:Si 1:1), this group was able to outnumber the abundance of non-silica dependent organisms such as dinoflagellates (5-30 %) and euglenophytes. This could be attributed to the ability of diatoms to make highly efficient use of short-lived pulses of silicic acid into the system, promoting the formation of thinner frustules and smaller diatom communities (Marchetti and Cassar, 2009). These pulses could be related to continental runoff and local resuspension of sediments (Torres et al., 2023), such as the observed at E8 (west to the Mackinlay constriction) where there is a shallowing of bottom depth (28 m), a reduction of seas surface salinity, low temperature most likely linked to the ventilation of deeper waters masses. At station 8 we were able to reach a N:Si close to 1, while N:P ratio reached its lowest 4.75, impinging a drawdown of nitrate by assimilation of primary producers. Nitrate+nitrite were scarce along the western section with N:P always below 10 (see Table 1), which is consistent with previous observations along the full extension of the BC (Giesecke et al., 2021).

Mean total-Nanoplankton abundance in the outer BC was almost the same as in the inner BC. E11 showed almost twice the abundance of nanoplankton than E13 (Fig. 4 B). As for most of the inner sector, in the outer BC (E11 and E13), nanoplankton was mainly represented by nanoflagellates (72 and 83 %) followed by diatoms (14 and 8 %), dinoflagellates and ciliates (*ca.* 2.5 %). Microplankton was less abundant (2 times) in the outer BC than in the inner BC (Fig. 4 C). At E11, microplankton was mainly represented by diatoms >20 µm. Whereas in E13, similar percentages of diatoms and dinoflagellates (*ca.* 45 %) were observed.

Nanoplankton at the mouth of BC was the highest, almost 3 times higher than in the inner and outer BC (Fig. 4 B), and was mainly represented by diatoms (70-80 %). Microplankton also presented the maximum registered values *ca*. 13 times higher than in the inner BC and 30 times of that registered in the outer BC. Microplankton was mainly represented by diatoms (55-97 %), similar to the inner BC, reaching the highest abundance of micro-sized diatoms (~10^5 cell L^{-1}), almost 10 times higher than the values recorded in the rest of the sampled sectors. This could be related to the transport of oceanic waters from Cape Horn Current (Acha et al., 2004), as mentioned above.

In general, small diatoms (<20 µm) were highly diverse and dominated by the genera *Chaetoceros* and *Thalassiosira*, while *Skeletonema* spp., *Leptocylindrus minimum*, *L. danicus*, *Cerataulina pelágica*, *Guinardia delicatula*, *Thalassionema nitzschioides* and *Navicula* spp., among others, were additionally frequent diatom species, similar as previously described by Almandoz et al., (2011). Dinoflagellates <20 µm were mainly

represented by the armored genera *Scrippsiella*, *Protoperidinium* and *Alexandrium*, and the unarmored *Gymnodinium* and *Amphidinium*, in coincidence with previous studies in the BC (Guinder et al., 2021).

Large diatoms (>20 µm) belonged to the genera *Chaetoceros*, *Thalassiosira*, *Rhizosolenia* and *Pseudo-nitzschia*. Nonetheless, *Asterionellopsis glacialis* *Stephano*pyxis *turris, Ditylum brightwelli*, *Licmophora gracilis*, *G. delicatula, T. nitzschioides*, *Eucampia* sp. and *Nitzschia longissima* were also frequent. Large dinoflagellates included the armored genera *Ceratium*, *Protoperidinium* and *Dynophysis*, and the unarmored *Gyrodinium*, *Gymnodinium* and *Torodinium*.

Nano-sized (8.6×10^2 - 2.9×10^4 cell L^{-1}) and micro-sized (2.1×10^2 - 4×10^3 cell L^{-1}) aloricated ciliates were mainly represented by the genera *Mesodinium* spp. and *Laboea* spp. while loricate ciliates from the genus *Tintinnopsis* were always less abundant. High ciliates abundances usually occurred along with low diatom abundances and vice versa, as shown in several studies (Calbet and Landry, 2004; Irigoien et al., 2005; Posch et al., 2015). All the species identified in the present study are listed in Table A (Supplementary data); most of them have been previously described in the BC (Almandoz et al., 2011; 2014; 2019; Iachetti, 2018; Benavides et al., 2019; Guinder et al., 2020), revealing a consistent composition between different years.

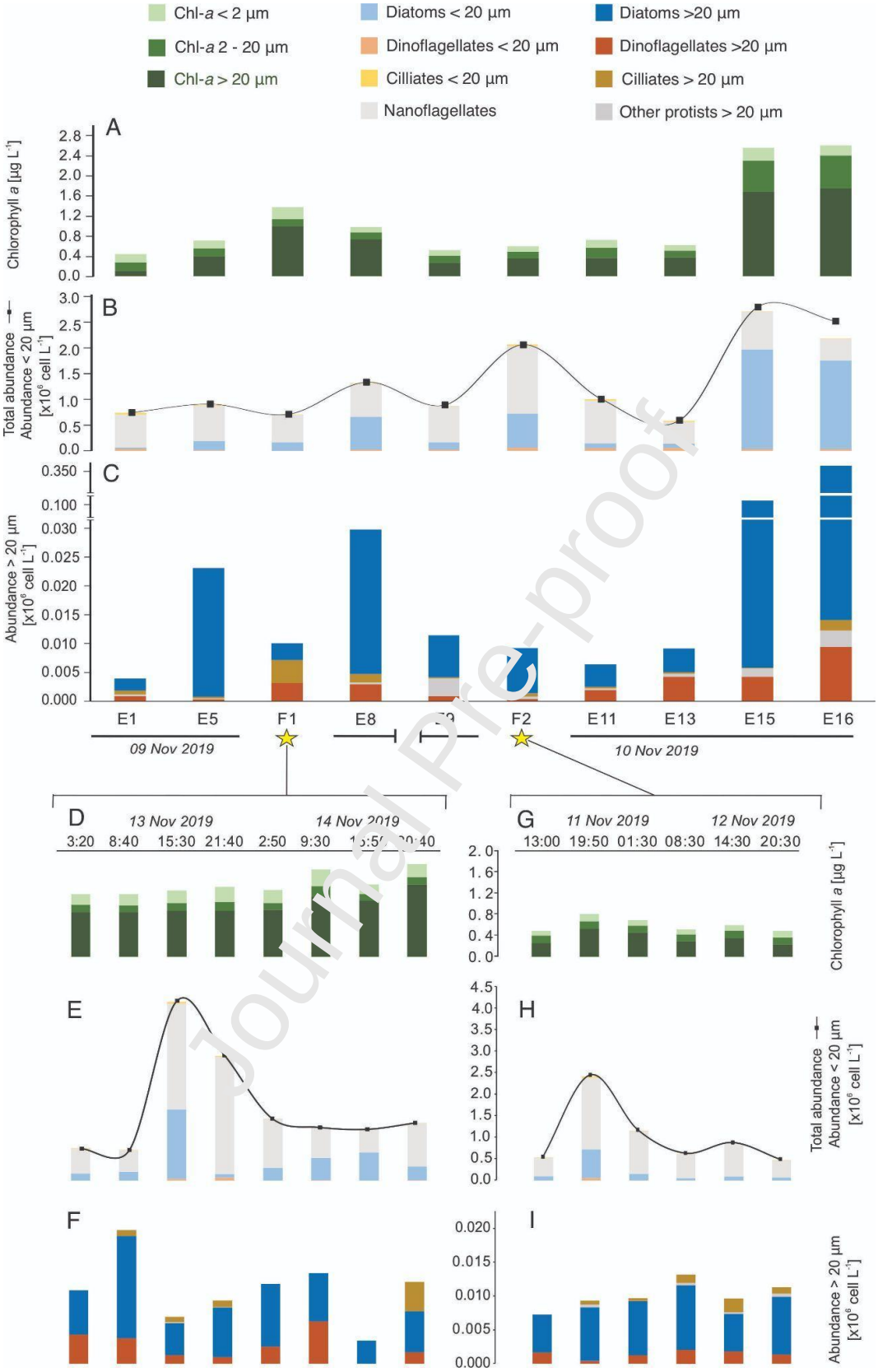

Figure 4. Chl-*a* size-fractions (in µg L^{-1}) (A, D, G) at the sampling stations, considering surface to maximum Chl-a waters (0-32 m) and plankton abundance (in cell L^{-1}) of nano- and microplankton (B, C, E, F, H, I). Figures A to C show all the sampled stations

longitudinally, whereas D to F and G to I are from the fixed stations, F1 and F2, respectively. As in Figure 1, stations sampled on the way back to Ushuaia (E to W transect) are indicated with yellow stars. Black lines in B, E and H show total plankton abundances (>2 μm). FULL PAGE

3.2. Temporal variability

While very rapid (*i.e.*, in the scale of hours) variation in meteorological conditions in the BC is a well-known feature to locals, this is the first time such an observation and its effect on plankton community are documented. Changes in temperature and wind speed were observed during the 6 days cruise. Air temperature increased from 3.5 (Table 1) to around 10 ºC (Table 2) from the beginning to the end of the cruise, while in 42 h, wind speed decreased from ~30 (Table 1) to 5 km h^{-1} (Table 2). Consequently, the first sampled stations in the inner BC (E1, E5, E8) were characterized by higher wind speed and lower air temperature (Table 1) than the same area on the way back to Ushuaia (F1, Table 2). Then, when reaching the outer BC (stations E9, E11, E13) air temperature was higher and wind speed lower, and this trend was even more marked, mainly for air temperature, when the same area was visited on the way back to Ushuaia (F2, Table 2). Such rapid changes affected surface waters characteristics and changes might be further reflected in the plankton community.

Table 2. Summary of environmental and hydrological variables during the studied period for eastern Beagle Channel. 24 h-averaged air temperature and wind speed, Median values for water temperature (T_W), salinity (S), density sigma theta (σ_t) and averaged values ± standard deviation for nutrient concentration, for surface to maximum Chl-a (0-32 m) waters for the different sampling sites at fixed stations F1 and F2 and the average (av). S.date, sampling date. Bot depth, bottom depth. MLD, mix layer depth.

Station	S. date	Bot. depth (m)	MLD (m)	T_{AIR} (ºC)	W. speed (km h^{-1})	T_W (ºC)	S	σ_t	PO_4 (μmol L^{-1})	NO_3+NO_2 (μmol L^{-1})	N:P
E.F2-T0	11 and 12 Nov 2019	28	20	12.07	16.68	6.53	31.37	24.62	1.075	5.247	4.856
E.F2-T6			4	10.84	24.80	6.51	31.14	24.44	1.07	5.35	5.08
E.F2-T12			16	9.56	24.88	6.55	31.40	24.64	1.20	5.21	4.33
E.F2-T18			10	8.74	23.88	6.61	31.50	24.71	1.01	7.32	7.08
E.F2-T24			10	9.02	19.00	6.58	31.44	24.67	1.17	7.85	6.60
E.F2-T30			14	9.16	16.08	6.68	31.27	24.53	1.17	9.28	7.88
F2 (av ± sd)			**12**	**10.65 ±2.88**	**18.93±13 .08**	**6.22 ±0,0 3**	**31.03 ±0,03**	**24.3± 0,02**	**1.12±0. 11**	**6.71±2.63**	**5.97± 2.07**

E.F1-T0	13 and 14 Nov 2019	182	8	9.44	13.00	6.94	31.00	24.28	1.07	3.71	3.48
E.F1-T6			5	9.80	12.72	6.97	31.03	24.30	1.04	7.28	7.03
E.F1-T12			67	10.28	13.56	6.87	31.05	24.32	1.30	5.28	4.06
E.F1-T18			14	10.45	12.84	7.39	31.00	24.22	0.86	6.32	7.50
E.F1-T24			5	10.16	13.60	6.89	31.05	24.32	1.14	5.25	4.66
E.F1-T30			9	9.96	16.40	7.42	30.88	24.12	1.09	5.82	5.31
E.F1-T36			5	9.89	16.00	7.14	30.99	24.24	1.05	5.18	4.97
E.F1-T42			6	9.75	14.48	7.03	31.04	24.30	0.85	2.57	2.68
F1 (av ± sd)			**15**	**9.99± 2.73**	**14.17±10 .32**	**7.10 ±0,0 0**	**31.04 ±0,11**	**24.28 ±0,04**	**1.03±0. 21**	**5.55±1.29**	**4.37± 1.56**

3.2.1. Outer BC - Fixed station F2

In F2 Air temperature increased from about 4.8 to 12 ºC from the time of sampling at E9 to the start of F2. Similarly, surface water temperatures were higher than those recorded two days before in the outer BC (Fig. 4 A), rapidly responding to the described changes in air temperature (Table 2). While air temperature decreased again by 3 ºC in the 30 h sampling-cycle in F2, sea water temperatures remained rather constant. (Fig. 5 E). Salinity was lower in surface waters (*ca*. 31.25) than in deeper waters (~32, Fig. 5 F) and no strong stratification was evident, and only observed at the beginning of the sampling-cycle (November 11 13:00 h, MLD = 20 m, Table 2). Coincidentally, the highest Chl-*a* concentrations and total plankton abundance at F2 (see below), were observed at the same time. Haline stratification was probably disrupted by wind driven vertical mixing of the water column, as wind speed reached its maximum values (*ca*. 25 km h^{-1}, Table 2).

On average, NO_3+ NO_2 concentrations at F2 were about half those of E9 (Table 2), but steady winds probably kept nutrient levels more or less constant, except when biological uptake was evident. $SiOH_4$ concentrations were below detection limit in surface waters of F2 during the whole sampling cycle. Total CTD-chl-*a* (Fig. 5 G) was <0.85 µg L^{-1} during the 30 h sampling cycle, reaching its maximum value in the first 6 h, in relation with the presence of nano-sized organisms (see below). Compared to plankton abundance in E9, higher total abundance in F2 most probably accounted for higher nutrient consumption. Towards the end of the sampling cycle, chl-*a* decreased and NO_3+NO_2 concentration was stable, probably as a result of the continuing wind resuspension and lower uptake by phytoplankton.

As in the W-E transect, chl-a_{TOT} was mainly represented by the largest size-fraction, chl-$a_{>20\mu m}$ (*ca*. 55 %), followed by the chl-$a_{2\text{-}20\mu m}$ fraction (20-30 %) and lastly chl-$a_{0.7\text{-}2\mu m}$ fraction (around 15-25 %) (Fig. 4 G). Chl-a_{TOT} (0.5 - 1 µg L^{-1}) as well as total plankton (>2 µm) abundance values (9.6 x 10^5 cell L^{-1} - 4.8 x 10^6 cell L^{-1}) in F2 were similar to those detected in the outer BC. However, chl-a_{TOT} and total plankton abundance increased rapidly during the first 6 h (19:50, November 11, Fig. 4 G and H), when small diatoms and nanoflagellates peaked (6.6 x 10^5 cell L^{-1} and 1.6 x 10^6 cell L^{-1}, respectively), along with ciliates (2.7 x 10^4 cell L^{-1}). Large diatom' abundance increased from 3.6 x 10^4 cell L^{-1} to 9.3 x 10^4 cell L^{-1}, six hours after ciliates declined (1.2 x 10^3 cell L^{-1} Fig. 4 I). On the next sampling events planktonic abundance decreased as mentioned previously for chl-*a.* Despite nutrient resuspension occurring in relation with wind mixing particles and sediment resuspension (Speroni et al., 2003), this may induce changes in light conditions in surface waters, *i.e.,* increase in turbidity (Flores Melo et al., 2018) and light limitation, as shown in other coastal areas (Schloss et al., 2002). Therefore, nutrient and sediment resuspension merit further studies in order to determine the relative importance of both processes in plankton dynamics.

Short-term variability in the composition of phytoplankton assemblages in coastal ecosystem have been previously reported (Pitcher et al., 1992; Côté and Platt, 1983; Pannard et al., 2008), some of them related to tidal cycles (Jouenne et al., 2007; Pannard et al., 2008; Affe et al., 2019). During this study period, tidal height ranged between 0.41 and 1.81 m. (Fig. 5), which is within the previously described mean height of 1.2 m (Balestrini et al., 1998). However, no effect of tidal regime was evident on plankton composition in F2. Although a clear warming of the surface water was observed, there is hardly any change in water masses that could explain plankton variability (Supplementary data Fig. A). However, water inflow cannot be ruled out, but no data are available to confirm this.

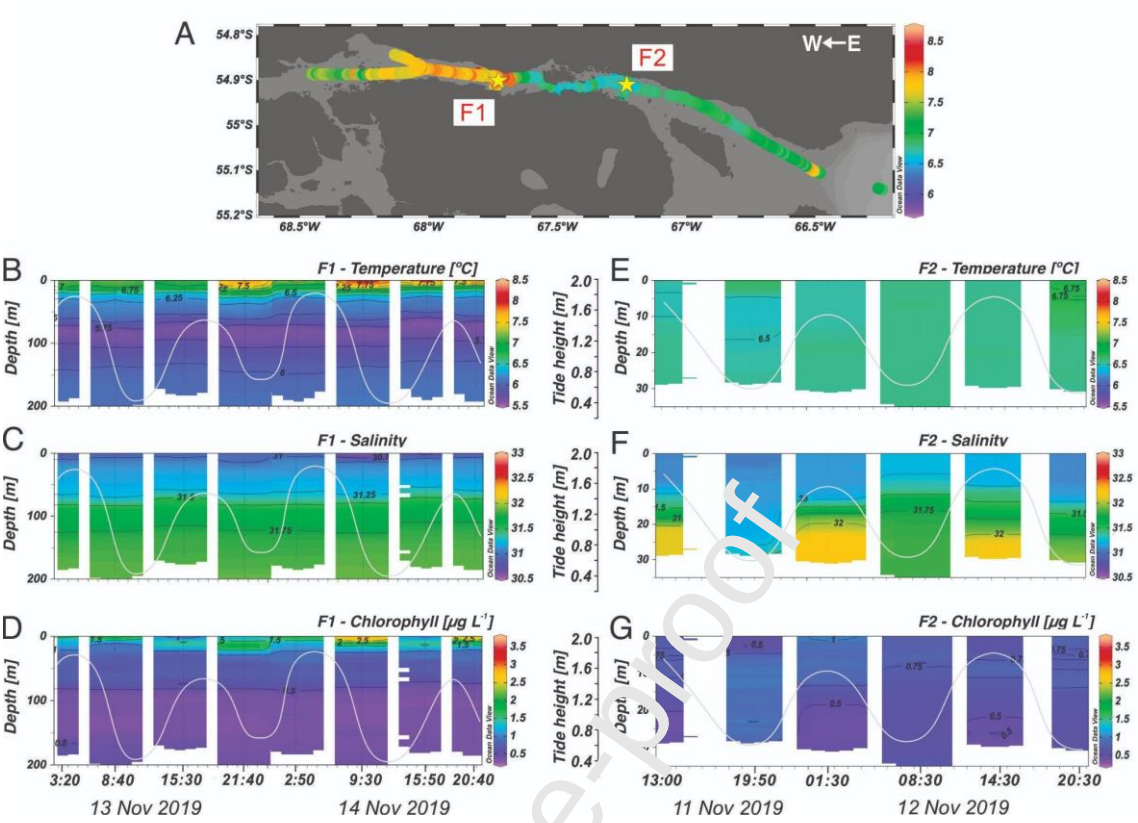

Figure 5. Surface continuous water temperature (A) along the E to W transect and CTD profiles for the different sampled times at both fixed stations F1 (B-D) and F2 (E-G); (B, E) Water temperature (ºC), (C, F) Salinity and (D-G) Chlorophyll-*a* (µg L^{-1}) (based on calibrated fluorescence data). Continuous white line depicts the tidal height. Sampling stations are indicated for better understanding. 1/3 PAGE

3.2.2. Inner BC - Fixed station F1

As in F2, air temperature increase led to an increase in surface water temperature (Table 2), reaching the highest recorded value in this study after 30 h, and coinciding with the low tide sampling of November 14 (9:30 h, Fig. 5 B). However, surface layer warming did not propagate to deeper layers nor changes in salinity could be observed during the same sampling period (Fig. 5 C), reinforcing the hypothesis that no water displacement occurred. No tidal effect can be inferred from this data, also stated by Martin et al. (2023). MLD values in F1 (*ca.* 15 m, Table 2) were within the range of those observed five days earlier in the inner BC; at the beginning of the 30 h sampling MLD <9 m (Table 2). The highest MLD value (67 m, Table 2) was registered on the second high tide cycle, after the first 12 h, as wind speed increased. This deepening of the MLD, and consequently, the mixing of the surface waters, could probably explain the changes in plankton abundance and composition occurred at this time (see below). Water temperature and salinity were relatively uniform (7.10 ± 0.00, 31.04 ± 0.11, respectively),

suggesting that these water masses were probably not affected by tidal cycles over this short-term period.

PO_4 and particularly, NO_3+NO_2 concentrations at F1 were lower than those of inner BC (E1, E5), sampled 5 days earlier (Table 2). This is probably due to nutrient uptake by >20 µm planktonic organisms, which increased their abundances at this time (see below).

Discrete chl-a_{TOT} (1.2 - 1.78 µg L^{-1}) values were mainly related to the largest size-fraction, chl-$a_{>20µm}$ (*ca.* 75 %) followed by the chl-$a_{0.7\text{-}2µm}$ fraction (15-20 %) and lastly the chl-$a_{2\text{-}20µm}$ fraction (5-15 %, Fig. 4 D). Chl-*a* concentration values in F1 doubled those from five days earlier. Similarly, the maximum total plankton abundance reached in F1 (on November 13, 16:00 h; 8.2 x 10^6 cell L^{-1}, Fig. 4 E, F) was one order of magnitude higher than maximum in inner BC, suggesting rapid plankton accumulation, with the dominance of small diatoms and nanoflagellates. The highest picophytoplankton biomass was also observed at this time during our cruise (Latorre et al., 2023; Malits et al., 2023). Moreover, dissolved oxygen concentration, which increased as the cruise advanced, reached its maximum values at F1, most probably related to an increase in primary production and a positive plankton community metabolic balance (Latorre et al., 2023). Large diatoms peaked at 10:00 h on November 13 (1.5x10^4 cell L^{-1},Fig. 4 F), decreasing 6 hours later and being replaced by small diatoms and nanoflagellates (1.6x10^6 cell L^{-1} and 2.4x 10^6 cell L^{-1}, respectively). At this time ciliates reached their maximum abundance (4.1x10^4 cell L^{-1}) after, possibly, grazing on large diatoms. Nanoflagellates were dominant 12 h later, at 22:00 h (2.7x10^6 cell L^{-1}), when small diatom abundance declined. High ciliates abundances occurred simultaneously with low diatom abundances and vice versa. Temporal changes in plankton abundance and composition during the 42 h (three tidal cycles) sampled, are well reflected in the total plankton trend but not in the chl-*a*, probably because a replacement among the dominant groups occurred without a major change in total biomass.

Similar rapid increases in biomass have been observed in response to meteorological and hydrographical short-term variability in other areas (Pitcher et al., 1992; Madariaga 2002; Yeager et al., 2005; Pannard et al., 2008). In the present study, the increase in both air and surface water temperature probably triggered phytoplankton primary production and growth, as shown by Latorre et al (2023), further fueled by the increase in silicic acid previously described for E8. While the intrusion of a different water mass in the area could be a possibility, the relatively low current velocities (Martin et al., 2023) and the high residence times described for the area, particularly for the waters west of Mackinlay Strait (around 50-60 days, Cucco et al., 2022), would indicate favor

phytoplankton growth in the same water mass as a response to the increase in stability and warming temperatures (Fig. A, Supplementary data).

Tidal related mixing processes can further influence species composition directly via the introduction of new species and indirectly altering water temperature, nutrient concentration and salinity (Pannard et al., 2008). In Bahía Blanca Estuary, Guinder et al. (2009) found relatively higher abundances of nano- and micro sized diatoms such as *Thalassiosira* spp and *Chaetoceros* spp during high tide, while smaller (nano-sized), solitary species without cell projections, presented higher abundances around low tide. The authors suggested that some features such as the cell size, shape, life style (chains *vs*. solitary cells), the ability to aggregate or disaggregate and the sinking rates could explain this phenomenon. Even if in F1 nano sized *Chaetoceros* spp. seem to be more abundant at diurnal high tides (data not shown), as in Guinder et al. (2009), our results are not conclusive to relate this short-term variability to the tidal cycle. On the other hand, Bahia Blanca Estuary has a tidal amplitude of 2.4 m (Pierini et al., 2009), higher than in our study (tidal amplitude = 1.4 m), which could explain the strong influence of tides on plankton dynamics in that area. As mentioned, changes in temperature probably triggered changes in the plankton metabolic balance (Latorre et al., 2023), resulting in higher chl-*a* concentrations on the last 30 to 42 h of sampling (10-16 h, 14 Nov, Fig. 5 D). Even if plankton abundances decreased (Fig. 4, E-F), chl-a_{TOT} continued increasing (Fig. 4 D). A peak in gross primary production (GPP, Latorre et al., 2023) measured at that time suggests that phytoplankton cells were metabolically active, accumulating pigments before dividing, which resulted in a relatively high chl-a_{TOT}/cell ratio. In addition, picoplankton increased in this station (Malits et al., 2023), but this group was not included in cell quantification during the present study, therefore offering an alternative explanation to the observed chl-a_{TOT} to cell ratio. Cellular duplication showed a delay with respect to the peak in GPP observed between 10-16 h. The duplication rate estimated for *C. didymus*, the most abundant species in the present study, was 1.6 d^{-1}, which is higher than values previously published (0.6 to 0.8 d^{-1}, Arteaga et al., 2020), suggesting that cells are growing in optimal conditions and that the time expected to duplicate biomass is about the same 10-16 h.

Hydrographic spatial variability found along the channel (PCA, Fig. 3, see section 3.1.) was only partially reflected in plankton community composition and distribution. Results of the nMDS (Supplementary Data, Fig. B) and ANOSIM test ($R_{ANOSIM} > 0.50$, $p < 0.05$) separated the mouth of BC (Group 1: E15-E16), characterized, as mentioned above, by the highest diatom abundances from the rest of the stations. Samples from stations E8 and F2 (Group 2), which could be defined as transition between the inner and outer channel, were characterized by similar total plankton abundances and

composition (as shown in section 3.2.1) and were grouped together, even if F2 was sampled on the way back, 2 days after station E8. Samples from stations E1, E5 and F1 (inner BC) as well as stations E9, E11 and E13 (outer BC) were grouped together (Group 3), clearly in relation with the dominance of nanoflagellates. However, even if F1 was part of Group 3, it was separated from the other stations in this cluster, probably due to the higher total plankton abundance. These results coincide with previously described differences associated with inner, and outer regions for the BC, *i.e.* west and east to Mackinlay Strait (Iachetti et al., 2021; Schloss et al., 2023, Malits et al., 2023). However, the fact of finding stations east and west of Mackinlay Strait grouping together here is related to the short period of the present study, and not to the long-term physico-chemical variables (or a single species abundance, as in Schloss et al., 2023). In this case, the relatively homogeneous plankton composition seems to be controlled by the timing of the ecological succession, rather than by the regionalization.

4. CONCLUSION

Subantarctic environments are known for their rapidly varying plankton assemblages over relatively short distances (Iachetti et al., 2021) . Understanding the factors that drive their distribution and abundance is key to understanding the health and productivity of marine ecosystems. One of the main factors that contribute to the rapid variability of plankton assemblages in sub-Antarctic environments is the physical environment, which can promote changes in water temperature, salinity, and nutrient availability, which in turn can influence the distribution and abundance of plankton. Another important factor only partially mentioned in the present study is biological interactions. Planktonic organisms, such as phytoplankton and zooplankton, form complex food webs that are shaped by predation, competition, and other ecological interactions, such as grazing by microzooplankton (ciliates). These interactions can vary over short distances and time scales, leading to rapid changes in the composition and abundance of plankton assemblages as observed in F1. In summary, the rapidly varying plankton assemblages in sub-Antarctic environments are influenced by a complex interplay of physical and biological factors.

Despite the challenges of studying plankton in sub-Antarctic environments, there have been significant advances in recent years in our understanding of their distribution and ecology. Advances in satellite remote sensing, molecular techniques, and autonomous underwater vehicles have provided new tools for studying plankton at high spatial and temporal resolutions. These advances have revealed the importance of small-scale processes and interactions in shaping plankton assemblages in different environments. In the present study, we observed important changes in species relative

abundance on a time scale of a few hours and days, which means that some important ecological processes (*e.g*. peaks in the abundance of toxic species) may be missed with a monthly sampling strategy. Sampling strategies should reflect the diverse scales of variability existent in planktonic processes in the BC, which could help to improve our ability to manage water quality or the accuracy of predictive models on bloom formation and decay and its influence on food webs. Moreover, the possible future implementation of aquaculture in the BC, reinforces the need to understand this highly dynamic and rapidly changing system, including its short-term variability.

Acknowledgements:

Authors thank G. Ferreyra and H. González Estay for their leadership in the overall project and the cruise, as well as the three scientific leaders of the cruise (A. Cabreira, R. Giesecke and M. Diez). We further thank the Pampa Azul Initiative from the Ministry of Science, Technology and Innovation and the National Council for Scientific and Technical Research (CONICET), grant RES-2019-2020-APN-DIR#CONICET, the National Institute of Fisheries Research and Development, as well as the crew of the R/V Víctor Angelescu. This work was also funded by the Prince Albert II Foundation, grant N° 2863, Argentinian National Law 26.875 fund (partial funding of ship time), the Ministries of Foreign Affairs of Argentina and Chile, Coast Guard Service of Argentina and the Chilean Navy for logistic support, in addition to FONDAP- IDEAL grant 15150003. Authors would also acknowledge the Gabinete de Oceanografía Física - Base Regional de Datos Oceanográficos (BaRDO) of the National Institute of Fisheries Research and Development. Authors kindly acknowledge Allison Cusick, as a native English speaker, for reading through this manuscript.

References:

Acha EM, Mianzan HW, Guerrero RA, Favero M, Bava J, 2004. Marine fronts at the continental shelves of austral South America: physical and ecological processes. Journal of Marine Systems 44 (2004), pp. 83–105.

Affe HM de J, Piedras FR, Lucineide MS, Oliveira Moser GA, Menezes M, de Castro Nunes JM, 2019. Phytoplankton functional groups: Short-term variation in a tropical tidal-forced estuarine system. Marine Ecology 40, e12555. https://doi.org/10.1111/maec.12555.

Alder V, Morales CE, 2009. Manual de métodos para el estudio de los sistemas planctónicos marinos. Eudeba. 268 pp.

Almandoz GO, Hernando MP, Ferreyra GA, Schloss IR, Ferrario ME, 2011. Seasonal phytoplankton dynamics in extreme southern South America. Journal of Sea Research 66 (2), 47–57. https://doi. org/10.1016/j.seares.2011.03.005.

Almandoz GO, Montoya NG, Hernando MP, Benavides HR, Carignan MO, Ferrario ME, 2014. Toxic strains of the *Alexandrium ostenfeldii* complex in southern South America (Beagle Channel, Argentina). Harmful Algae 37, 100–109. https://doi.org/10.1016/j.hal.2014.05.011.

Almandoz GO, Cefarelli AO, Diodato S, Montoya NG, Benavides HR, Carignan M, Hernando M, Fabro E, Metfies K, Lundholm N, Schloss IR, Álvarez M, Ferrario ME, 2019. Harmful phytoplankton in the Beagle Channel (South America) as a potential threat to aquaculture activities. Marine Pollution Bulletin 145, 105–117. https://doi.org/10.1016/j.marpolbul.2019.05.026 PMID: 31590766

Alvarez-Cobelas M, Rojo C, Benavent-Corai J, 2019. Long-term phytoplankton Dynamics in a complex temporal Realm. Scientific Reports, nature research 9(2019),15967. https://doi.org/10.1038/s41598-019-52333-z

Amo YD, Pape OL, Treguer P, Queguiner B, Menesguen A, Aminot A, 1997. Impacts of high-nitrate freshwater inputs on macrotidal ecosystems. I. Seasonal evolution of nutrient limitation for the diatom-dominated phytoplankton of the Bay of Brest (France). Marine Ecology Progress Series 161, 213–224.

APHA/AWWA/WEF, 1999. Standard Methods for the Examination of Water and Wastewater method 4500-P-F (1999 forward).

APHA/AWWA/WEF, 2000. Standard Methods for the Examination of Water and Wastewater, APHA/AWWA/WEF, method 4500 SiO2– D, method 4500-NO3-F (2000 forward).

Arrigo KR, van Dijken GL, Bushinsky S, 2008. Primary production in the Southern Ocean, 1997–2006. Journal of Geophysical Research 113 (2008), C08004, 10.1029/2007JC004551.

Arteaga LA, Boss E, Behrenfeld MJ, Westberry TK, Sarmiento JL, 2020. Seasonal modulation of phytoplankton biomass in the Southern Ocean. Nature Communications 11:5364. https://doi.org/10.1038/s41467-020-19157-2.

Balestrini C, Manzella G, Lovrich GA, 1998. Simulación de Corrientes en el Canal Beagle y Bahía Ushuaia mediante un Modelo Bidimensional. Reporte Técnico N 98. Buenos Aires, Servicio de Hidrografía Naval, pp. 1–58.

Barrera F, Lara RJ, Krock B, Garzón-Cardona JE, Fabro E, Koch BP, 2017. Factors influencing the characteristics and distribution or surface organic matter in the

Pacific-Atlantic connection. Journal of Marine Systems 175, 36–45. https://doi.org/10.1016/j. jmarsys.2017.07.004.

Baars JWM, 1981. Autecological investigations on marine diatoms. 2. Generation times of 50 species. Hydrobiological Bulletin 15(1981), 137–151. https://doi.org/10.1007/BF02255172.

Benavides HR, Montoya NG, Carignan MO, Luizón C, 2019. Environmental features and Harmful Algae in an area of bivalve shellfish production of the Beagle Channel, Argentina. Marine and Fishery Science 32, 71–101. https://doi.org/10.47193/ mafis.3222019121901.

Boyd PW, 2002. Environmental factors controlling phytoplankton processes in the Southern Ocean. Journal of Phycology 38 (2002), 844–861. https://doi.org/10.1046/j.1529-8817.2002.t01-1-01203.x

Calbet A, Landry M, 2004. Phytoplankton growth, microzooplankton grazing, and carbon cycling in marine systems. Limnology and Oceanography 49, 51–57.

Cardona-Garzón JE, Martínez AM, Barrera F, Pfaff F, Koch BP, Freije RH, Gómez EA, Lara RJ, 2016. The Pacific-Atlantic connection: Biogeochemical signals in the southern end of the Argentine shelf. Journal of Marine Systems 163, 95–101. https:// doi.org/10.1016/j.jmarsys.2016.07.006.

Carranza MM, Gille ST, 2015. Southern Ocean wind-driven entrainment enhances satellite chlorophyll-a through the summer. Journal of Geophysical Research: Oceans 120, 304– 323, doi:10.1002/2014JC010203.

Chisholm, S.W., 1992. Phytoplankton Size. In: Falkowski, P.G., Woodhead, A.D., Vivirito, K. (Eds.), Primary Productivity and Biogeochemical Cycles in the Sea. Springer, US, Boston, MA, pp. 213–237.

Clarke KR, Warwick RM, 1994. Similarity-based testing for community pattern: the two-way layout with no replication. Marine Biology 118, 167–176.

Clarke KR, Gorley RN. 2006. PRIMER v6: User Manual/Tutorial., Plymouth: PRIMER E.

Cloern JE, 1991. Tidal stirring and phytoplankton bloom dynamics in an estuary. Journal of Marine Research 49, 203–221.

Côté B, Platt T, 1983. Day-to-day variations in the spring–summer photosynthetic parameters of coastal marine phytoplankton. Limnology and Oceanography 28, 320–344.

Cucco A, Martín J, Quattrocchi G, Fenco H, Umgiesser G, Fernández DA, 2022. Water Circulation and Transport Time Scales in the Beagle Channel, Southernmost Tip of South America. Journal of Marine Science and Engineering 10 (2022), 941. https://doi.org/10.3390/jmse10070941

Cuevas, L.A., Tapia, F.J., Iriarte, J.L., González, H.E., Silva, N. and Vargas, C.A., 2019. Interplay between freshwater discharge and oceanic waters modulates phytoplankton size-structure in fjords and channel systems of the Chilean Patagonia. Progress in Oceanography, 173, pp.103-113.

EPA, 1993. Methods for the Determination of Inorganic Substances in Environmental Samples, EPA 600/R93/100, August 1993; Method 353.2, Revision 2.0. (nitrites, nitrates).

Flores-Melo X, Martin J, Romero S, Durrieu De Madron X, Bourrin F, Malits A, Rodriguez-Flores CN, Rivello Lopez G, Chiarandinni J, 2018. Patrones Oceanográficos a lo largo del Canal Beagle Argentino durante el invierno austral. X Jornadas Nacionales de Ciencias del Mar. FCEyN, UBA. Buenos Aires.

Flores Melo X, Martín J, Kerdel L, Bourrin F, Colloca CL, Menniti C, de Madron XD, 2020. Particle dynamics in Ushuaia Bay (Tierra del Fuego)-Potential effect on dissolved oxygen depletion. Water (Switzerland) 12, 324. https://doi.org/ 10.3390/w12020324.

Flores-Melo X, Giesecke R, Martín J, Schloss IR, Latorre, MP, Durrieu de Madron X, Bourrin F, Spinelli M, Menniti C, González HE, Menschel E, Martín, J. n.d. Downward fluxes of particulate matter in the Beagle Channel: seasonal and spatial variability. Journal of Marine Systems. This issue.

Garreaud RD, Vuille M, Compagnucci R, Marengo J, 2009. Present-day South American climate. Palaeogeography, Palaeoclimatology, Palaeoecology 281, 180–195. https:// doi.org/10.1016/j.palaeo.2007.10.032v.

Geider R, La Roche J, 2002. Redfield revisited: variability of C:N:P in marine microalgae and its biochemical basis, European Journal of Phycology 37(1), 1-17.https://doi.org/ 10.1017/S0967026201003456

Giesecke R, Martín J, Pinoñes A., Hofer J, Garcés-Vargas J, Flores-Melo X, Alarcón E, Durrieu de Madron X, Bourrin F, González HE, 2021. General Hydrography of the Beagle Channel, a Subantarctic Interoceanic Passage at the Southern Tip of South America. Frontiers in Marine Science 8, 621822 https://doi.org/10.3389/ fmars.2021.621822.

González, H.E., Calderón, M.J., Castro, L., Clement, A., Cuevas, L.A., Daneri, G., Iriarte, J.L., Lizárraga, L., Martínez, R., Menschel, E. and Silva, N., 2010. Primary production and plankton dynamics in the Reloncaví Fjord and the Interior Sea of Chiloé, Northern Patagonia, Chile. Marine Ecology Progress Series, 402, pp.13-30.

González, H.E., Graeve, M., Kattner, G., Silva, N., Castro, L., Iriarte, J.L., Osmán, L., Daneri, G.and Vargas, C.A., 2016. Carbon flow through the pelagic food web in

southern Chilean Patagonia: relevance of Euphausia vallentini as a key species. *Marine Ecology Progress Series*, *557*, pp.91-110.

Guinder V, Popovich CA, Perillo GME, 2009. Short-term variability in the phytoplankton and physico-chemical variables in a high-tidal regime, Bahía Blanca Estuary, Argentina. Brazilian journal of oceanography, 57(3), 249–258.

Guinder VA, Malits A, Ferronato C, Krock B, Garzón-Cardona J, Martínez A, 2020. Microbial plankton configuration in the epipelagic realm from the Beagle Channel to the Burdwood Bank, a Marine Protected Area in Sub-Antarctic waters. PLoS ONE 15(5), e0233156. https://doi.org/10.1371/journal.pone.0233156

Harris GP, 1980.Temporal and Spatial Scales in Phytoplankton Ecology.' Mechanisms, Methods, Models, and Management. Canadian Journal of Fisheries and Aquatic Sciences 37, 877–900.

Harris V, Edwards M, Olhede SC, 2014. Multidecadal Atlantic climate variability and its impact on marine pelagic communities. Journal of Marine Systems 133 (2014) 55–69.

Iachetti CM, 2018. Fluctuación temporal de la estructura de la comunidad microbiana planctónica en la zona eufótica del Canal Beagle (Tierra del Fuego, Argentina). PhD *Thesis , Facultad de Ciencias Exactas y Naturales, Universidad de Buenos Aires, 166 pp*.

Iachetti CM, Lovrich G, Alder VA, 2021. Temporal variability of the physical and chemical environment, chlorophyll and diatom biomass in the euphotic zone of the Beagle Channel (Argentina): Evidence of nutrient limitation. Progress in Oceanography 195, 102576. https://doi.org/10.1016/j.pocean.2021.102576.

Iriarte JL, Kusch A, Osses J, Ruiz M, 2001. Phytoplankton biomass in the sub-Antarctic area of the Straits of Magellan (53°S), Chile during spring-summer 1997/1998. Polar Biology 24 (2001), 154-162.

Iriarte, J.L., Pizarro, G., Troncoso, V.A. and Sobarzo, M., 2000. Primary production and biomass of size-fractionated phytoplankton off Antofagasta, Chile (23–24 S) during pre-El Nino and El Nino 1997. Journal of Marine Systems, 26(1), pp.37-51.

Iriarte JL, Cuevas LA, Cornejo F, Silva N, González HE, Castro L, Montero P, Vargas CA, Daneri G, 2018. Low spring primary production and microplankton carbon biomass in Sub-Antarctic Patagonian channels and fjords (50– 53°S). Arctic, Antarctic and Alpine Research, 50, e1525186. https://doi.org/10.1080/15230430.2018.1525186.

Irigoien X, Flynn KJ, Harris RP, 2005. Phytoplankton blooms: a 'loophole' in microzooplankton grazing impact?. Journal of Plankton Research 27(4), 313–321 https://doi.org/10.1093/plankt/fbi01.

Irion S, Christaki U, Berthelot H, L'Helguen S, Jardillier L, 2021. Small phytoplankton contribute greatly to CO2-fixation after the diatom bloom in the Southern Ocean. The ISME Journal 15 (2021), 2509–2522. https://doi.org/10.1038/s41396-021-00915-z.

Isla F, Bujalesky G, Coronato A, 1999. Procesos estuarinos en el canal Beagle, Tierra del Fuego. Revista de La Asociación Geológica Argentina 54(4), 307–318.

Iturraspe R, Sottini R, Schroeder C, Escobar J, 1989. Hidrología y Variables Climáticas del Territorio de Tierra del Fuego. Ushuaia: Información Básica vol. 7, 201.

Jäger CG, Diehl S, Schmidt GM, 2008. Influence of water-column depth and mixing on phytoplankton biomass, community composition, and nutrients. Limnology and Oceanography 53(6), 2361–2373. https://doi.org/10.4319/lo.2008.53.6.2361.

Jacob, B.G., Tapia, F.J., Daneri, G., Iriarte, J.L., Montero, P., Scharzo, M. and Quiñones, R.A., 2014. Springtime size-fractionated primary production across hydrographic and PAR-light gradients in Chilean Patagonia (41–50 S). Progress in Oceanography, 129, pp.75-84.

Jouenne F, Lefebvre S, Véron B, Lagadeuc Y, 2007. Phytoplankton community structure and primary production in small intertidal estuarine-bay ecosystem (eastern English Channel, France). Marine Biology 151, 805–825.

Käse L, Geuer JK, 2018. Phytoplankton responses to marine climate change–an introduction. In Jungblut S, Liebich V, Bode M (Eds). YOUMARES 8–Oceans Across Boundaries: Learning from each other, pages 55–72, Springer. https://doi.org/10.1007/978-3-319-93284-2_5.

Latorre MP, Berghoff CF, Giesecke R, Malits A, Pizarro G, Iachetti CM, Martin J, Flores Melo X, Gil MN, Iriarte JL, Schloss IR. n.d. Plankton metabolic balance in the Beagle Channel during spring. Journal of Marine Systems. This issue.

Leles SG, Alves de Souza C, Faria CO, Ramos AV, Alexandre Macedo Fernandes AM, de Oliveira Moser GA, 2014. Short-term phytoplankton dynamics in response to tidal stirring in a tropical estuary (Southeastern Brazil). Brazilian Journal of Oceanography 62(4), 341–349.

Lopes CB, Lillebo AI, Dias JM, Pereira E, Vale C, Duarte AC, 2007. Nutrient dynamics and seasonal succession of phytoplankton assemblages in a Southern European European Estuary: Ria de Aveiro, Portugal. Estuarine, Coastal and Shelf Science 71, 480–490.

Lucas LV, Cloern JE, 2002. Effects of Tidal Shallowing and Deepening on Phytoplankton Production Dynamics: A Modeling Study. Estuaries 25(4A), 497–507.

Malits A, Monforte C, Iachetti C, Gerea M., Latorre M., 2023. Source characterization of dissolved organic matter in the eastern Beagle Channel from a spring situation. Journal of Marine Systems. This issue.

Madariaga I, 2002. Short-term variations in the physiological state of phytoplankton [2pt] in a shallow temperate estuary. Hydrobiologia 475–476, 345–358.

Marchetti, A., & Cassar, N. (2009). Diatom elemental and morphological changes in response to iron limitation: a brief review with potential paleoceanographic applications. Geobiology, *7*(4), 419-431.

Martín J, Alonso G, Dragani W, Meyerjürgens J, Giesecke R, Cucco A, Fenco H (2023). General circulation and tidal wave propagation along the Beagle Channel, Journal ofMarine Systems, https://doi.org/10.1016/j.jmarsys.2023.103889

Martín J, Malits A, Kreps G, Flanagan R, Iachetti CM, Lovrich GA, 2016. Procesos oceanográficos e implicaciones ambientales en un pasaje interoceánico subpolar: El Canal Beagle (Tierra del Fuego, Argentina). V Simposio Internacional de Ciencias Del Mar, 207–208.

Mojica KD, van de Poll WH, Kehoe M, Huisman J, Timmermans KR, Buma AG, et al., 2015. Phytoplankton community structure in relation to vertical stratification along a north-south gradient in the Northeast Atlantic Ocean. Limnology and Oceanography 60, 1498–521.

Pannard A, Claquin P, Klein C, Le Roy B, Véron B, 2008. Short-term variability of the phytoplankton community in coastal ecosystems in response to physical and chemical conditions' changes, Estuarine, Coastal and Shelf Science 80 (2008), 212–224. https://doi.org/10.1016/j.ecss.2008.08.008.

Parsons TR, Maita R, Lalli CM, 1984. Counting, Media and Preservation. A Manual of Chemical and Biological Methods for Seawater Analysis. Pergamon Press, Toronto. Alder VA, Morales CE. 2009. Manual de métodos para el estudio de los sistemas plantónicos marinos. Buenos Aires, Argentina: Eudeba.268pp.

Pierini J, Gómez O, Eduardo A, 2009. Tidal forecasting in the Bahia Blanca Estuary, Argentina Interciencia, 34 (12), 851–856.

Pitcher GC, Brown PC, Mitchell-Innes BA, 1992. Spatio-temporal variability of phytoplankton in the southern Benguela upwelling system, South African Journal of Marine Science, 12(1), 439–456. 10.2989/02577619209504717.

Posch T, Eugster B, Pomati F, Pernthaler J, Pitsch G, Eckert EM, 2015. Network of interactions between ciliates and phytoplankton during spring. Frontiers in Microbiology 6. 10.3389/fmicb.2015.01289.

Reynolds CS, 1990. Temporal scales of variability in pelagic environments and the response of phytoplankton. Freshwater Biology 23 (1990), 25-5.

Savidge G, Boyd P, Pomroy A, Harbour D, Joint I, 1995. Phytoplankton production and biomass estimates in the northeast Atlantic Ocean, May–June 1990. Deep Sea Res Part I: Oceanogr Res Pap Deep Sea Res I. 42, 599–617.

Schloss IR, Ferreyra GA, Ruiz-Pino D, 2002. Phytoplankton biomass in Antarctic shelf zones: a conceptual model based on Potter Cove, King George Island. Journal of Marine Systems 36 (2002), 129–143.

Schloss IR, Wasilowska A, Dumont D, Almandoz GO, Hernando MP, Michaud-Tremblay CA, Saravia L, Rzepecki M, Monien P, Monien D, Kopczyńska EE, Bers AV, Ferreyra GA, 2014. On the phytoplankton bloom in coastal waters of southern King George Island (Antarctica) in January 2010: An exceptional feature? Limnology and Oceanography 59(1), 195–210.

Schloss IR, Pizarro G, Cadaillon AM, Giesecke R, Hernando M, Almandoz G, Latorre M, Malits A, Flores-Melo X, Saravia L, Martín J, Guzmán L., Iachetti C, Ruiz C, 2023. Spatial dynamics of HABs and toxins distribution along the Beagle Channel. Journal of Marine Systems. This issue.

Speroni JO, Dragani WC, Mazio CA. Mediciones de Co rrien e en Paso Mackinlay, Canal Beagle, Tierra del Fuego, De- partamento Oceanografia, Informe Tecnico 1/3. 2003. Available online: https://www.researchgate.net/publication/312613566_Simulacion_de_corrientes_en_el_Canal_Beagle_y_Bahia_Ushuaia_mediante_un_modelo_bidimensional

Swart S, Thomalla SJ, Monteiro PMS, 2015. The seasonal cycle of mixed layer dynamics and phytoplankton biomass in the Sub- Antarctic Zone: A high-resolution glider experiment. Journal of Marine Systems 147, 103–115. doi:10.1016/j.jmarsys.2014.06.002.

Thomalla SJ, Fauchereau N, Swart S, Monteiro PMS, 2011. Regional scale characteristics of the seasonal cycle of chlorophyll in the Southern Ocean. Biogeosciences 8 (2011). pp. 4763-4804.

Thyssen M, Mathieu D, Garcia N, Denis M, 2008. Short-term variation of phytoplankton assemblages in Mediterranean coastal waters recorded with an automated submerged flow cytometer. Journal Of Plankton Research, 30 (9), 1027–1040.

Tomas CR, 1997. Identifying marine phytoplankton. 858 pp.

Torres, R., Silva, N., Reid, B. and Frangopulos, M., 2014. Silicic acid enrichment of subantarctic surface water from continental inputs along the Patagonian archipelago interior sea (41–56 S). Progress in Oceanography, 129, pp.50-61.

Torres R, Reid B, Frangópulos M, Alarcón E, Márquez M, Häussermann V, Försterra G, Pizarro G, Iriarte JL, González HE, 2020. Freshwater runoff effects on the production of biogenic silicate and chlorophyll-a in western Patagonia archipelago (50–51°S). Estuarine, Coastal and Shelf Science 241(December 2019). https://doi.org/10.1016/j.ecss.2020.106597

Uitz J, Claustre H, Griffiths FB, , Ras J, Garcia N, Sandroni V, 2009. A phytoplankton class-specific primary production model applied to the Kerguelen Islands region (Southern Ocean). Deep-Sea Research I 56 (2009), 541–560.

USEPA, 1983. Methods for Chemical Analysis of Waters and Wastes, USEPA 600/4-79-020, 1983: Method 370.1.

USEPA, 1993. Methods for the Determination of Inorganic Substances in Environmental Samples, USEPA 600/R 93/100, August 1993: Method 365.1, Rev. 2.0.

Utermöhl H, 1958. Zur vervollkommnung der quantitativen phytoplankton-methodik. Mitteilung Internationale Vereinigung für Theoretische unde Angewandte Limnologie. 9, 1–38

Valdenegro A, Silva N, 2003. Características oceanográficas físicas y químicas de la zona de canales y fiordos australes de Chile entre el estrecho de Magallanes y cabo de Hornos (CIMAR 3 Fiordos). Ciencia y Tecnología Marina 26, 19–60.

Ward BB, Van Oostende N, 2016. Phytoplankton assemblage during the North Atlantic spring bloom assessed from functional gene analysis. Journal of Plankton Research 38,1135–50.

Wetz MS, Hayes KC, Lewitus AJ, Wolny JL, White DL, 2006. Variability in phytoplankton pigment biomass and taxonomic composition over tidal cycles in a salt marsh estuary. Marine Ecology Progress Series 320, 109–120.

Yeager CLJ, Harding, LW, Mallonee ME, 2005. Phytoplankton production, biomass and community structure following a summer nutrient pulse in Chesapeake Bay. Aquatic Ecology 39, 135–149.

Declaration of interests

☒ The authors declare that they have no known competing financial interests or personal relationships that could have appeared to influence the work reported in this paper.

☐The authors declare the following financial interests/personal relationships which may be considered as potential competing interests:

Highlights

Highlight 1: Spatial variability in microphytoplankton was observed along the Beagle Channel (BC)

Highlight 2: Phytoplankton assemblages were related to bathymetry, temperature, and macronutrients

Highlight 3: Fast changes in plankton were related to growth rather than advection of water masses

Highlight 4: Temperature and wind speed affected both chl-a concentration and phytoplankton growth

Highlight 5: This is the first work to report such high temporal variability in plankton in the BC